Supporting Information

Scale-up of slurry Taylor flow microreactor for heterogeneous photocatalytic synthesis of azo-products

Runjuan Du[a,b,1], *Yuhang Chen*[a,b,1], *Zhiming Ding*[a,b], *Chuanting Fan*[a,b], *Gang Wang*[a,b], *Jie Zhang*[a,b,*] *and Zhiyong Tang*[a,b,c,d*]

[a]CAS Key Laboratory of Low-Carbon Conversion Science and Engineering, Shanghai Advanced Research Institute, Chinese Academy of Sciences, Shanghai, 201210, PR China

[b]School of Chemical Engineering, University of Chinese Academy of Sciences, Beijing, 100049, PR China

[c]School of Chemistry and Material Science, University of Science and Technology of China, Hefei, Anhui, 230026, PR China

[d]Key Laboratory of Functional Molecular Solids, Ministry of Education, Anhui Engineering Research Center of Carbon Neutrality, College of Chemistry and Materials Science, Anhui Normal University, Wuhu 241000, PR China

---

[1] Contributed equally to this work

*Corresponding authors

Contact info: zhangjie@sari.ac.cn (J. Zhang); tangzy@sari.ac.cn (Z. Tang)

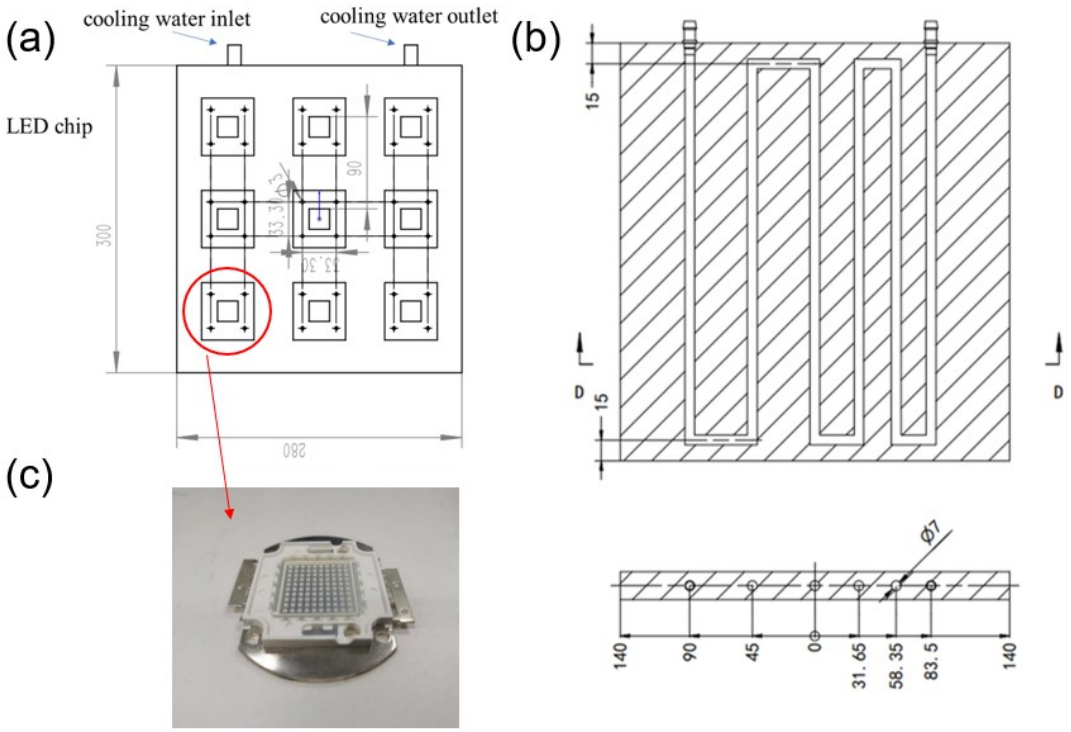

Fig. S1. Design of LED light source and its temperature control system.

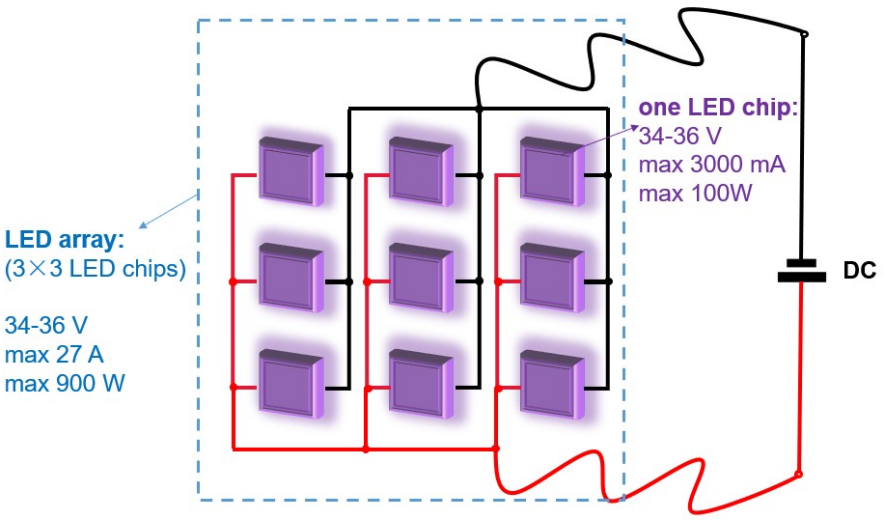

Fig. S2. Electrical settings of LED chips.

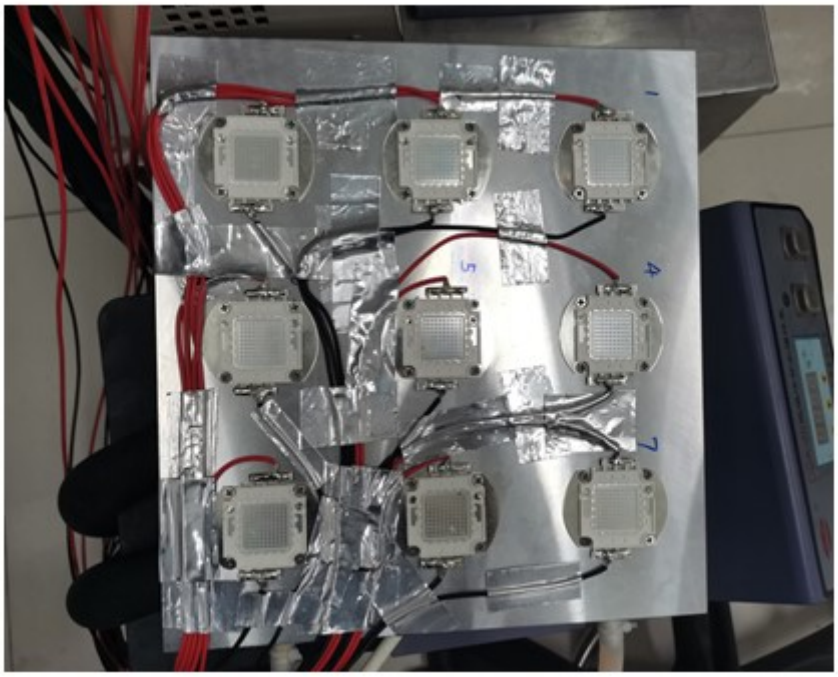

Fig. S3. The 100 W package LED chips used in the experiment.

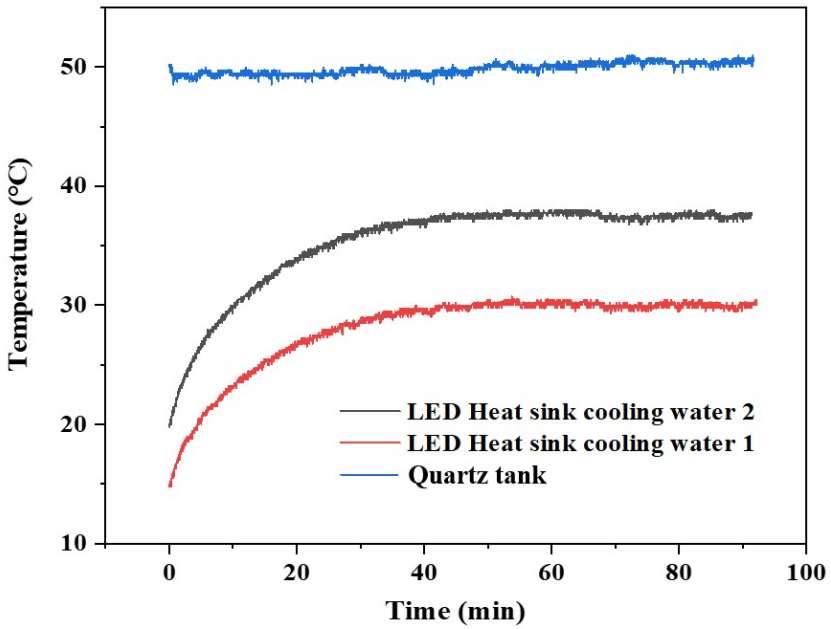

Fig. S4. The temperature variation in different areas during the stability test.

Note S1. CFD simulations of water-cooling system of LED light source

In this work, simulations were performed using COMSOL Multiphysics software to optimize the design and operation parameters of cooling system to achieve effective cooling. Some factors that have minor impact on the simulation results were ignored to speed up the simulation. The simplifications were as follows:

(1) The mathematical model of UV-LED cooling system only considered the heat conduction and thermal convection of the structural components, without considering the thermal radiation of the LED and the water-cooled components.

(2) The heat source is the LED chips in this whole system. To reduce the number of grids, it was simplified to a sheet structure with side length of 20 mm and the thickness of 0.5 mm according to the actual size of the LED chip.

(3) The contact thermal resistance between the copper substrate and the aluminum water-cooled heat sink was modeled by the equivalent thin layer thermal resistance in the COMSOL heat transfer module, with a thin layer thickness of 50 μm. The material was conductive silicone grease with a thermal conductivity of 3 W/ (m.K), in consistent with the experiment.

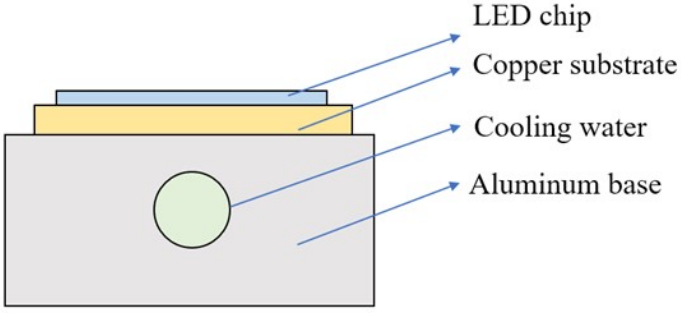

Fig. S5. Schematic diagram of simplified water-cooling model.

The 3D simulation model of LED light source and its water-cooling plate is shown in Fig. 2a, main manuscript. According to the calculated Reynold number in the cooling water pipe, the k-ε turbulence model was used during the simulation. Default parameters were selected for the turbulent kinetic energy and turbulent dissipation rate. For the heat transfer, the solid and fluid heat transfer modules were selected in COMSOL and multi-physics field coupling was applied to the non-isothermal flow.

The quality of the mesh dissection has an important influence on the simulation results. To achieve a reasonable dissection of the model, the maximum size of the mesh was set to 5 mm and the minimum size was set to 0.1 mm. The model after grid construction is shown in Fig. S6. The final total number of meshes was 764,000.

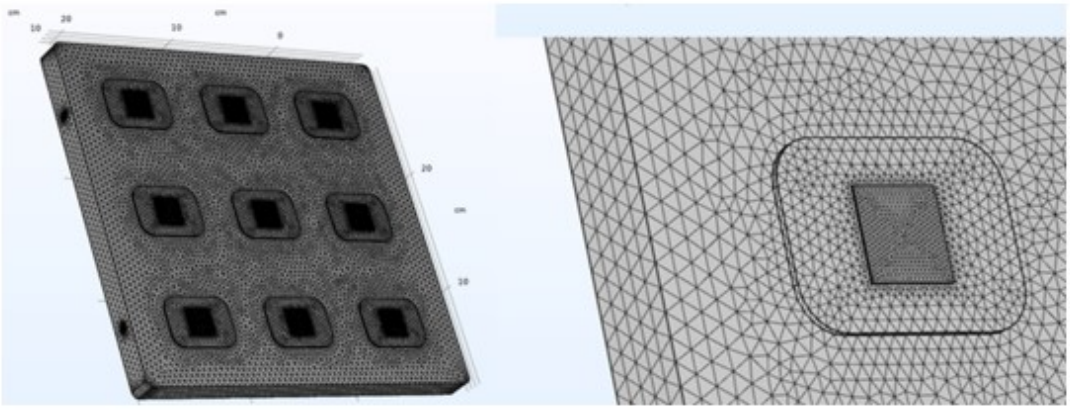

Fig. S6. The final model after grid construction.

The boundary conditions of the numerical simulation were as follows:

(1) 9 LED chips were set as the “heat source” with a heat generation rate P_0=1000 W.

(2) The initial ambient temperature was 20℃. The fluid inlet temperature was 10-30℃ and the inlet fluid flow rate was 5-7 m/s.

(3) Since the thermal radiation of the LED and water-cooling components were not considered, the copper base and aluminum water-cooled components surface were set to “thermal insulation”.

(4) The contact thermal resistance between the LED chip and the copper base was modeled by the equivalent thin layer thermal resistance model in the COMSOL heat transfer module, with a thin layer thickness of 5 μm. The material was silver gel with a thermal conductivity of 17.6 W/(m·K).

Fig. S7 shows the simulated temperature distribution in the LED chip and water-cooling substrate under the working conditions. It was found that the highest temperatures of LED chip were 35℃, which was 10℃ higher than its copper substrate. The cooling water stayed around 20°C, showing 5°C of maximum temperature gradient as compared to the aluminum substrate in the area below the LED chip.

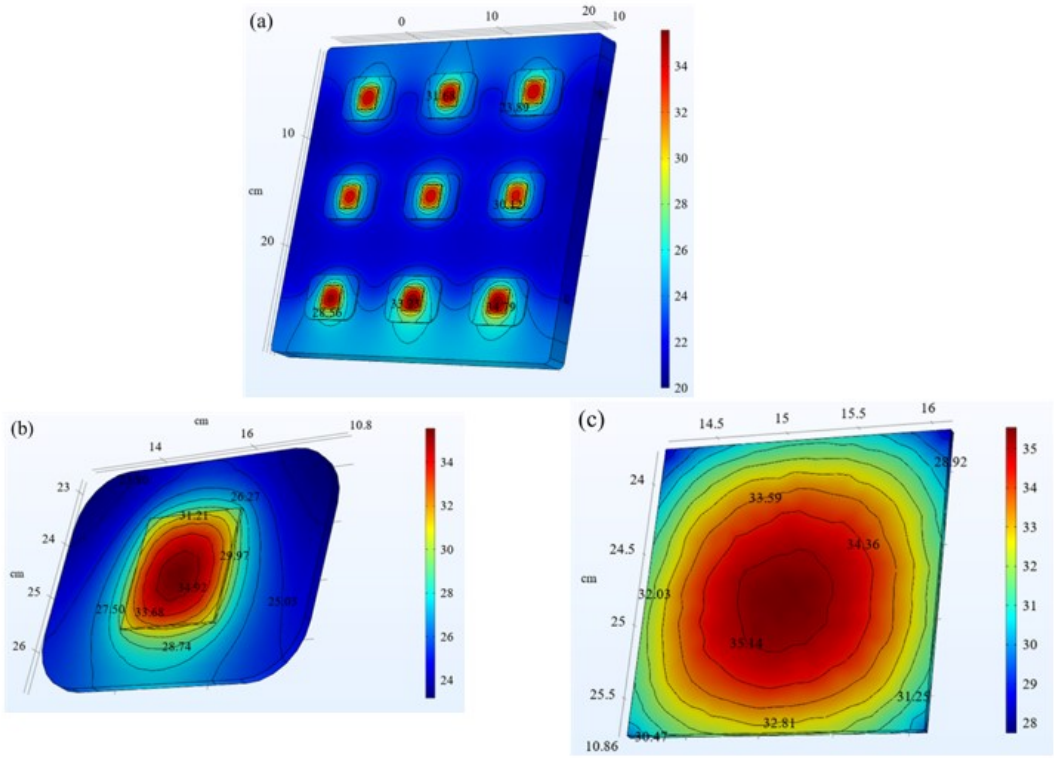

Fig. S7. The temperature distribution in the LED chip and water-cooling substrate (cooling water inlet flow rate 5 m/s, temperature 20℃).

The effect of the inlet temperature and flow rate of the cooling water on the surface temperature of the LED chip was further studied, and the results are shown in Fig. S8 and S9, respectively. When the cooling water inlet flow rate was 5.0 m/s, the cooling water inlet temperature had a greater effect on the chip surface temperature. When the cooling water temperature increased from 10℃ to 35℃, and the maximum temperature of the chip surface increased from 25.1℃ to 49.3℃. In contrast, the cooling water inlet flow rate has less influence on the chip surface temperature. When the inlet flow rate increased from 5.0 m/s (11.5 L/min) to 7.0 m/s (16.2 L/min), and the maximum chip temperature decreased from 35.1℃ to 34.3℃. Overall, the maximum temperature on the surface of LED chip always stayed blow 50°C with a cooling water temperature of

10-35℃ and a flow rate of 11.5-16.2 L/min, demonstrating the effectiveness of designed water-cooling plate.

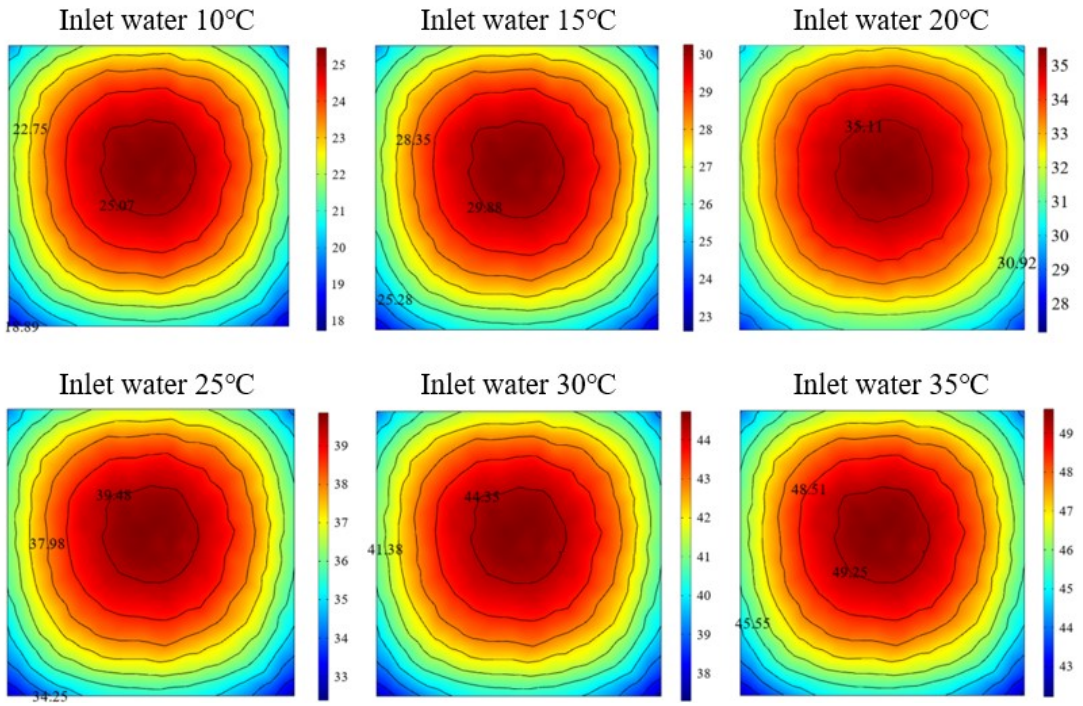

Fig. S8. The evolution of LED chip temperature with different cooling-water temperatures (cooling-water inlet flow rate 5 m/s).

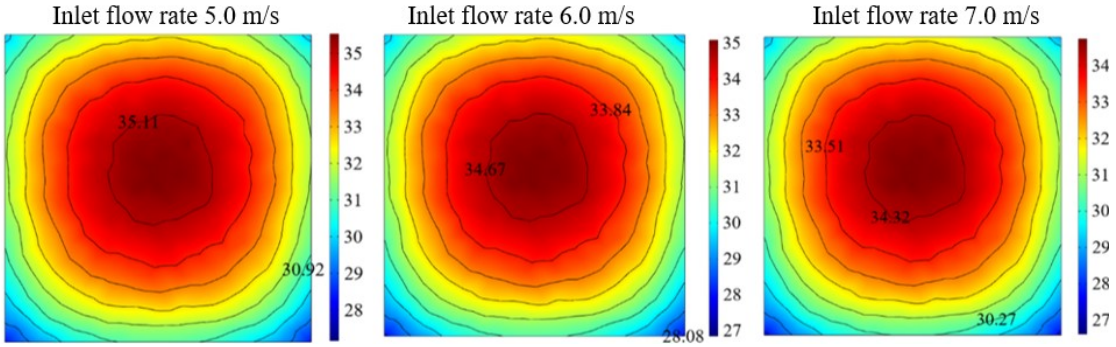

Fig. S9. The evolution of LED chip temperature with different inlet flow rates of cooling water (cooling-water inlet temperature 20℃).

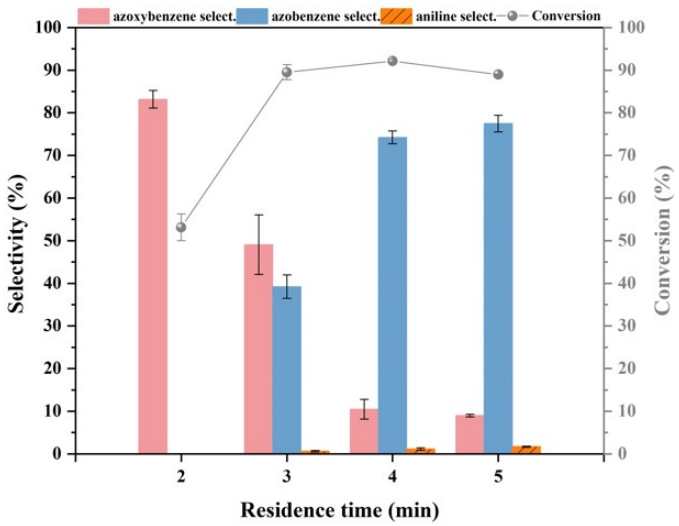

Fig. S10. Effect of residence time on the performance of photocatalytic reaction, residence time was varied by changing the total flow rate (reaction conditions: substrate concentration 8 mM, reaction temperature 50°C, g-C_3N_4 content 5 mg/mL, β_G = 0.4, total flow Q_{total}=50 mL/min, and LED electrical power=1800 W).

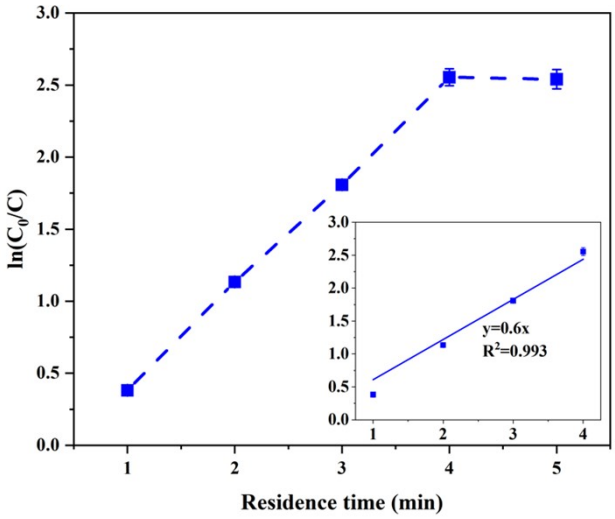

Fig. S11. The fitting of first-order reaction kinetics for photocatalytic conversion of nitrobenzene.

Note S2. Calculation of the apparent quantum yields (AQY) and Space-time yield (STY)

The apparent quantum yields (AQY) of the reaction was calculated using eq. S1.

$$AQY = \frac{N_{e-}}{N_{photon}} \times 100\% \quad \text{(S1)}$$

N_{e-} (/h) is the number of electrons consumed per hour as the reaction proceeds under certain operating conditions, which is calculated by eq. S2.

$$N_{e-} = \frac{\left[6 \cdot n_{(azoxybenzene)} + 8 \cdot n_{(azobenzene)} + 6 \cdot n_{(aniline)}\right] \cdot N_A \cdot 60}{10^3} \quad \text{(S2)}$$

where N_A is Avogadro's constant, 6.02×10^{23} /mol; $n_{(azoxybenzene)}$, $n_{(azoxybenzene)}$, and $n_{(aniline)}$ (mmol/min) are the numbers of molecules of azoxybenzene, azobenzene, and aniline produced per minute as the reaction proceeds under certain operating conditions, respectively (eq. S3). 6, 8 and 6 are the number of electrons transferred to produce one molecule of azoxybenzene, azobenzene and aniline, respectively.

The $n_{(azoxybenzene)}$, $n_{(azoxybenzene)}$, and $n_{(aniline)}$ were calculated as follows:

$$n_{(azoxybenzene)} = 0.5 \cdot c_{(nitrobenzene)} \cdot Q_{Total} \cdot (1 - \beta_G) \cdot conversion \cdot selectivity_{(azoxybenzene)} \cdot 10^{-3}$$

$$n_{(azobenzene)} = 0.5 \cdot c_{(nitrobenzene)} \cdot Q_{Total} \cdot (1 - \beta_G) \cdot conversion \cdot selectivity_{(azobenzene)} \cdot 10^{-3}$$

$$n_{(aniline)} = c_{(nitrobenzene)} \cdot Q_{Total} \cdot (1 - \beta_G) \cdot conversion \cdot selectivity_{(aniline)} \cdot 10^{-3} \quad \text{(S3)}$$

where, $c_{(nitrobenzene)}$ is the concentration of nitrobenzene before reaction, 8 mmol/L; Q_{Total} (mL/min) is the total flow rate; *conversion* donates the conversion of

nitrobenzene; $selectivity_{(azoxybenzene)}$, $selectivity_{(azoxybenzene)}$, and $selectivity_{(aniline)}$ are the selectivity of azoxybenzene, azobenzene and aniline, respectively.

N_{Photon} (/h) is the number of incident photons per hour reaching the reaction system upon irradiation at 405 nm, which was calculated by eq. S4.

$$N_{Photon}（405nm） = \frac{ES\lambda \times 3600}{hc} \quad \text{(S4)}$$

where, E (W/m^2) is the irradiation intensity. λ is the wavelength of the light source, 405 nm, i.e. 405×10^{-9} m. h is Planck's constant, 6.626×10^{-34} J·S. c is the speed of light, 2.998×10^8 m/s. S (m^2) is the area exposed to light, which was calculated by eq. S5.

$$S = 0.5 \times \pi dl \quad \text{(S5)}$$

Where, d is the inner diameter of the PFA capillary, 2.65×10^{-3} m. l is the length of the PFA capillary, 36.28 m.

The space-time yield (STY, g·L^{-1}·day^{-1}), which is defined as the amount of target products generated per unit volume of reactor per unit time, was calculated using eq. S6.

$$STY = \frac{0.5 \times 24 \times 60 \cdot Q_{total} \cdot （1 - \beta_G） \cdot c_{nitrobenzene} \cdot conversion \cdot \sum selectivity_i . M_i}{10^6 \cdot V_{reactor}} \quad \text{(S6)}$$

Where, M_i refers to the relative molecular mass of azoxybenzene and azobenzene, $M_{azoxybenzene}$=198.2, $M_{azobenzene}$=182.2; $V_{reactor}$ is the volume of the reactor, 0.2 L.

Furthermore, the moles of electrons involved in the reaction over a certain residence time (n_{e-}, mol) that is calculated using eq. S7. The moles of two target products (azoxybenzene and azobenzene) formed in the reaction over a certain residence time ($n_{products}$, mmol) that is calculated by eq. S8.

$$n_{e-} = \frac{\left[6 \cdot n_{(azoxybenzene)} + 8 \cdot n_{(azobenzene)} + 6 \cdot n_{(aniline)}\right] \cdot t}{10^3} \quad \text{(S7)}$$

$$n_{products} = t \cdot \left[n_{(azoxybenzene)} + n_{(azobenzene)}\right] \quad \text{(S8)}$$

Where, t is the residence time, min. $n_{(azoxybenzene)}$, $n_{(azoxybenzene)}$, and $n_{(aniline)}$ (mmol/min), are the moles of azoxybenzene, azobenzene, and aniline produced per minute as the reaction proceeds under certain operating conditions, respectively, which is calculated by eq. S3.

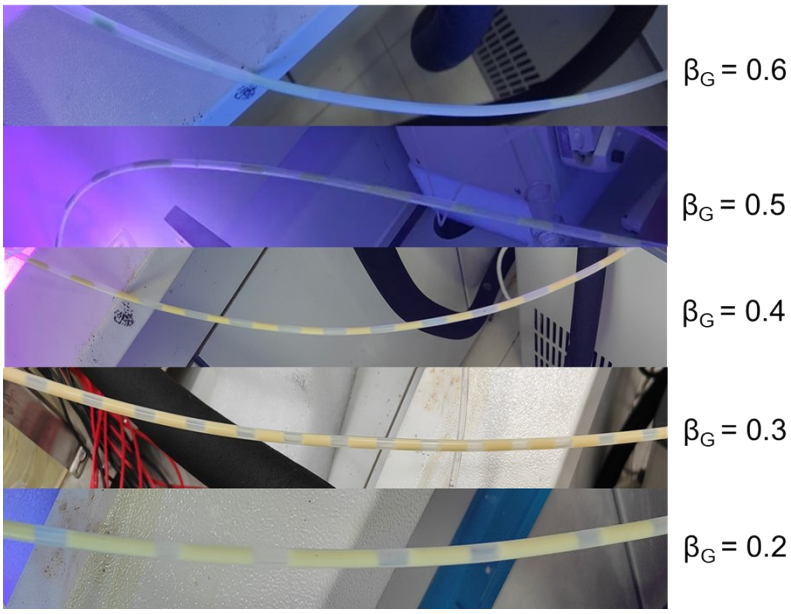

Fig. S12. Effect of gas fraction on the homogeneity and stability of slurry Taylor flow.

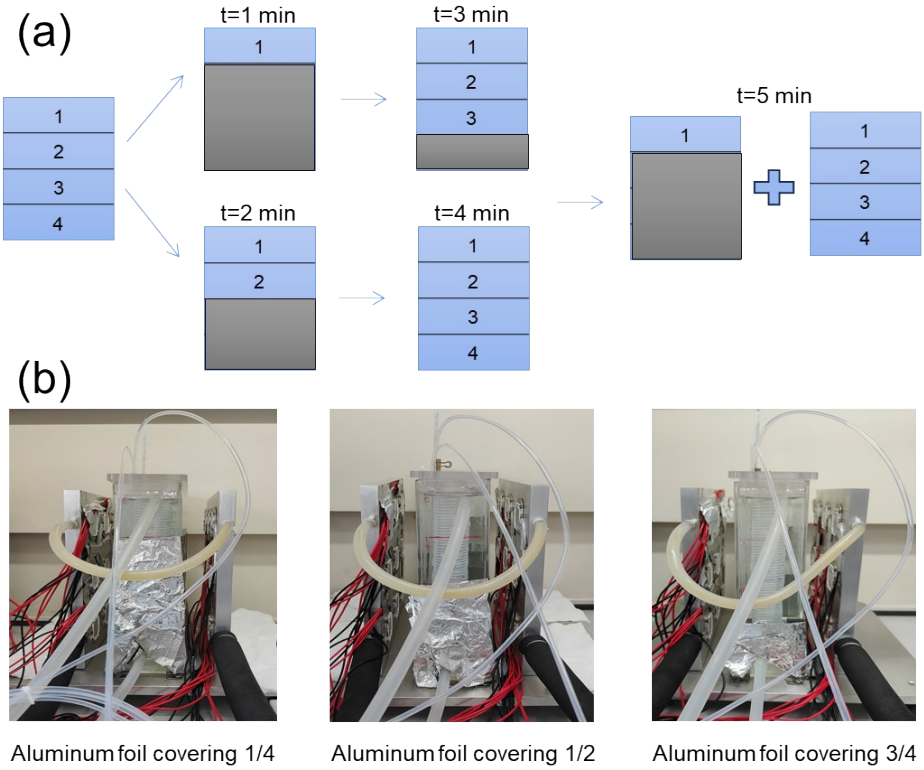

Fig. S13. A single-factor control on residence time using the masking method with aluminum foil: (a) schematic diagram, (b) experimental setup.

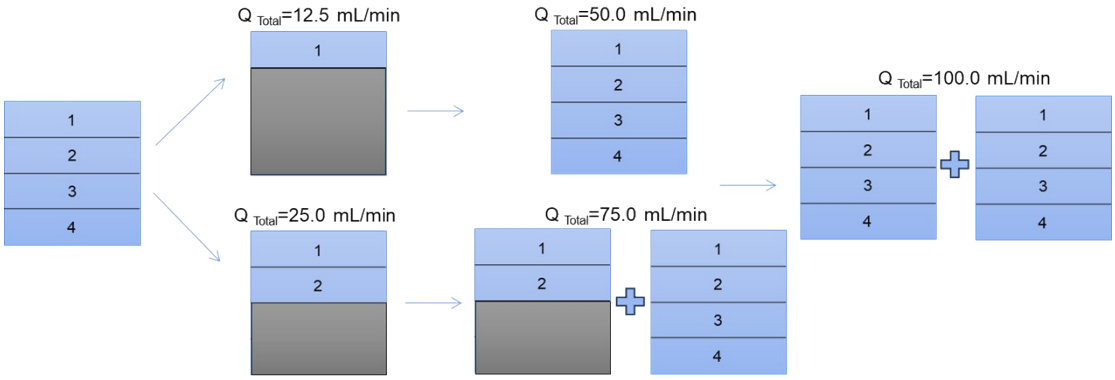

Fig. S14. A single-factor control on the total flow rate using the masking method with aluminum foil.

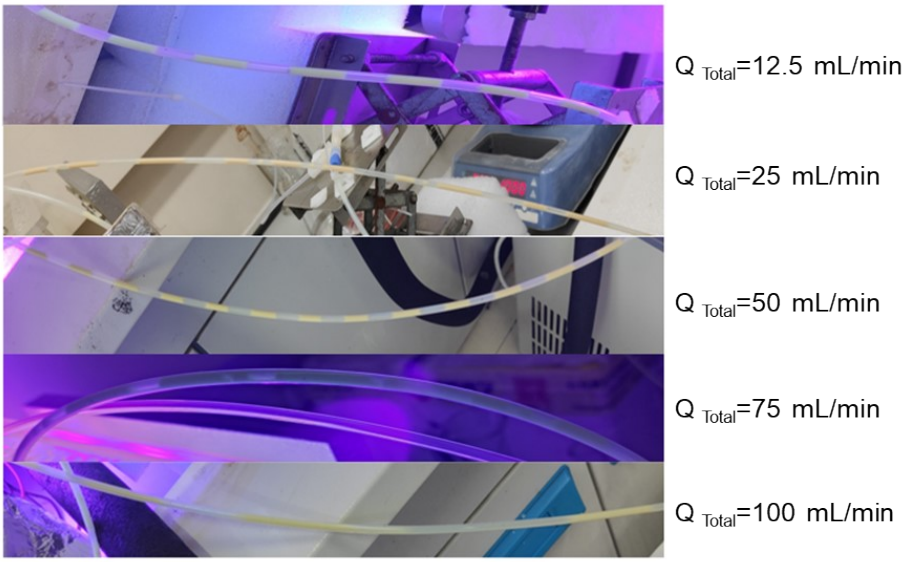

Fig. S15. Effect of total flow rate on the homogeneity and stability of slurry Taylor flow.

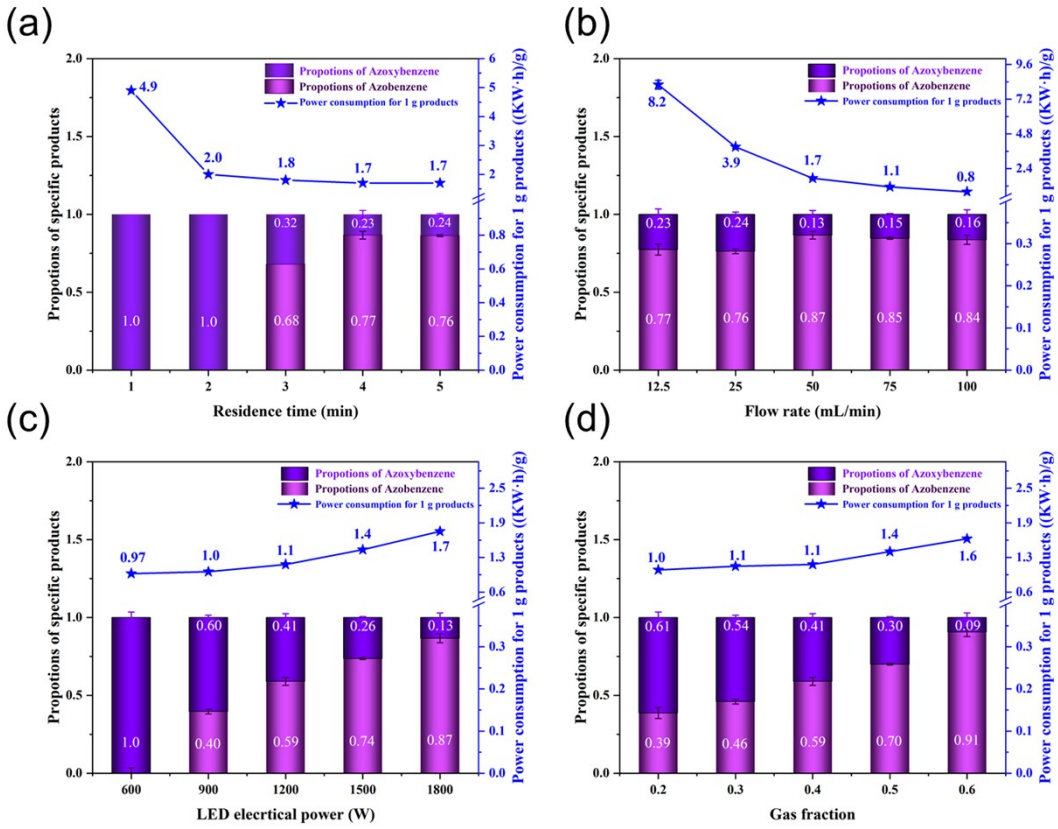

Fig. S16. The power consumption for synthetizing 1 g of azo-products (KW·h/g) and the relative content of azoxybenzene and azobenzene in 1g of products under different conditions: (a) Effect of residence time (reaction conditions: substrate concentration 8 mM, reaction temperature 50℃, g-C_3N_4 content 5 mg/mL, β_G = 0.4，total flow Q_{total}=50 mL/min, and LED electrical power =1800 W); (b) The effect of total flow rate(reaction conditions: substrate concentration 8 mM, catalyst content 5 mg/mL, gas fraction β_G = 0.4, and LED electrical power =1800 W); (c) Effect of LED electrical power (reaction conditions: substrate concentration 8 mM, reaction temperature 50℃, g-C_3N_4 content 5 mg/mL, residence time τ =4 min, β_G = 0.4, Q_{Total}=50 mL/min); (d) Effect of gas fraction (reaction conditions: substrate concentration 8 mM, catalyst content 5 mg/mL, reaction temperature 50℃, residence time τ =4 min, total flow Q_{total} =50 mL/min, and LED electrical power = 1200 W).